

The unit cell expansion of branched polyethylene as detected by Raman spectroscopy: an experimental and simulation approach

J. Otegui · J. F. Vega · S. Martín · V. Cruz ·
A. Flores · C. Domingo · J. Martínez-Salazar

Received: 14 November 2006 / Accepted: 30 November 2006 / Published online: 13 January 2007
© Springer Science+Business Media, LLC 2007

Raman spectroscopy has become a commonly used technique for the study of phase structure in semi-crystalline polymers [1–8]. Among them, polyethylene (PE) is one of the more deeply explored materials. However, there are still some remaining questions concerning the effect molecular and structural features in the intensity and position of characteristic Raman signals. The Raman crystallinity band appearing in linear PE at 1415 cm^{-1} is thought to arise from factor group splitting, where the two PE chains packed in the orthorhombic unit cell cause the CH_2 bending vibrational mode to split with a second component appearing at 1440 cm^{-1} [4, 9, 10]. The other characteristic band appearing at 1460 cm^{-1} has been shown to arise from superposition of rocking combination modes, which interact with the crystal mode with symmetry B_{3g} [11]. Changes in the crystalline phase, i.e. in the unit cell parameters for example as a result of temperature changes or the inclusion of short branches, could affect this phenomenon resulting on changes in the interchain energy interactions [8, 9]. The shift in the position of the 1415 cm^{-1} band towards a higher wavenumber observed as crystallinity decreases has been associated with a lower effectiveness of the interchain interaction

within the lattice, and hence to lateral disorder in the crystals. Lagarón has recently found a correlation between the shift of this crystalline band and the macroscopic density for a set of PE samples with different molecular architectures [8]. However, the variation did not result in a linear correlation, probably due to the molecular heterogeneity of the selected samples.

In this work we carried out a careful analysis of the orthorhombic crystalline band observed by Raman spectroscopy, i.e., the CH_2 bending 1415 cm^{-1} mode, as a function of crystal features obtained from X-Ray scattering (WAXS) and differential scanning calorimetry (DSC), for a series of model ethylene/1-hexene copolymers, with varying comonomer content, obtained in our laboratory from single-site catalyst polymerization (see Table 1). The materials are characterized by having a narrow molecular weight distribution ($M_w/M_n=2$) and a homogeneous comonomer distribution. The weight average molecular weight (M_w) of the samples ranges between 120 and 300 kg mol^{-1} . We will interpret the experimental shift observed in terms of the variations in the crystalline orthorhombic structure found in the materials. Moreover, we will compare the experiments with computed results calculated at the local Density Functional Theory (DFT) level. For that purpose, normal modes of vibration were obtained for the orthorhombic cells with different parameters derived from the X-ray data.

The splitting of the single-chain vibrational active modes into the bands at 1415 and 1440 cm^{-1} , can be observed in Fig. 1a for the linear PE sample. The separation between these two bands has been obtained for all polymers studied and listed in Table 1. The exact

J. Otegui · J. F. Vega (✉) · S. Martín ·
V. Cruz · A. Flores · J. Martínez-Salazar
Departamento de Física Macromolecular, Instituto de
Estructura de la Materia, CSIC Serrano 113 bis, Madrid
28006, Spain
e-mail: imtv477@iem.cfmac.csic.es

C. Domingo
Departamento de Física Molecular, Instituto de Estructura
de la Materia, CSIC Serrano 121, Madrid 28006, Spain

Table 1. Comonomer molar content (^{13}C -NMR), melting temperature (DSC), lattice parameters and crystallinity (WAXS), density and Raman CH_2 bending splitting separation of the samples studied

Sample	mol-% 1-hexene	T_m (°C)	a (nm)	b (nm)	X_c	ρ (kg/m 3)	CH_2 bending splitting separation (cm $^{-1}$)
EH0	0	134.2	0.7399 ± 0.0002	0.4942 ± 0.0001	0.70	952 ^a	22.9
EH3	0.56	125.9	0.7427 ± 0.002	0.4948 ± 0.0001	0.59	938 ^a	22.6
EH5	1.57	121.4	0.7444 ± 0.004	0.4954 ± 0.0001	0.53	931 ^a	22.2
EH8	1.62	120.7	0.7459 ± 0.006	0.4956 ± 0.0002	0.50	926 ^a	22.0
EH10	1.92	116.3	0.7478 ± 0.002	0.4962 ± 0.0001	0.48	922 ^a	21.7
EH15	3.20	103.5	0.753 ± 0.01	0.4973 ± 0.0004	0.34	908 ^b	21.3
EH23	5.10	99.0	0.757 ± 0.03	0.4977 ± 0.0008	0.25	891 ^b	20.6
EH35	8.30	75.4	0.759 ± 0.02	0.4980 ± 0.0005	0.16	879 ^b	20.0
EH42	10.1	66.8	0.763 ± 0.01	0.4983 ± 0.0003	0.09	871 ^b	19.8

^a Obtained from gradient column

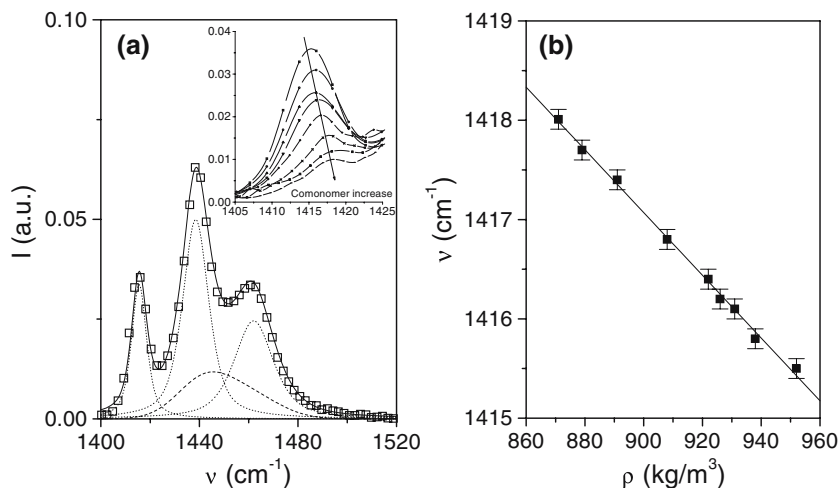
^b Calculated values based on crystallinity considering polyethylene crystalline density of 1000 kg/m 3 and amorphous density of 856 kg/m 3

positions have been obtained by a fitting procedure following the method proposed by Strobl and Hagedorn [1], and accounting for the amorphous contribution to the bending region. It is clearly seen in Table 1 that an increase in comonomer content gives rise to a smaller separation of the bands. It has been also observed (see the inlet to Fig. 1a) that the crystalline band at 1415 cm $^{-1}$ is the most sensitive one to changes in the crystalline phase [8]. The drop in the intensity is due to the progressive decrease in the crystalline content. At the maximum comonomer content the band seems to vanish almost completely. Figure 1b plots the position of this band as a function of the density of the samples. The band shifts towards higher wavenumber with decreasing density, in agreement with the results previously obtained by Lagarón [8]. The linear correlation found in this variation is excellent, likely due to the molecular homogeneity of the samples studied.

The cell parameters of the materials listed in Table 1 have been determined by a least squares fit of WAXS reflections at room temperature. It has been

reported in the literature that cell “ c ” axis does not depend of the type of material, and a nearly constant value of $c = 0.2542$ nm is obtained [12–15]. The unit cell parameters “ a ” and “ b ” increase as comonomer content does, but the changes in dimensions of unit cell are mostly due to the expansion of the a -axis (see Table 1). This means a lateral separation of the two interacting chains within the orthorhombic lattice [12–15]. This trend is expected and it has been related to a reduction in the lamellar thickness in ethylene-based copolymers, and then in the melting temperature (also listed in Table 1 for our materials) as it is expressed through the well-known Thomson–Gibbs equation. The changes observed in the splitting phenomenon should then directly be related to these variations of the crystal lattice. A decrease of the separation between the peaks at 1415 and 1440 cm $^{-1}$, and then the shift of the 1415 cm $^{-1}$ band, has been attributed to a decrease of the inter-chain interaction due to a lower crystal density induced by the presence of branches, and then higher unit cell volume [8, 9]. We have

Fig. 1 (a) Raman spectrum of linear PE in the $-\text{CH}_2-$ bending zone. The lines are the result of the fitting procedure following Strobl and Hagedorn [1] The inset shows the variations found in the 1415 cm $^{-1}$ crystalline band as comonomer content increases; (b) Position of the crystalline band as a function of density in the materials studied



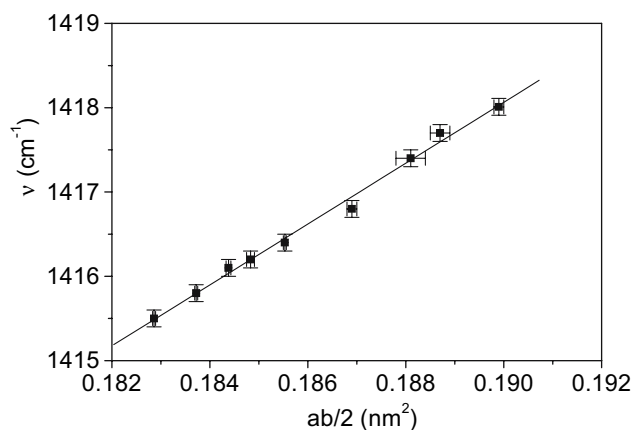


Fig. 2 Peak position of the 1415 cm^{-1} crystalline band vs the effective chain cross-section of orthorhombic cell obtained from WAXS measurements

plotted the change in the position of the crystalline band as a function of the cross-section of the orthorhombic unit cell, $ab/2$ in Fig. 2. The shift in 1415 cm^{-1} band follows a nice linear correlation with the change in the effective cross-section of the orthorhombic cell. These results are in agreement with those obtained by Lagarón et al., who related similar correlation between the CH_2 bending factor group splitting separation with density for polyketones [16].

Finally, the experimentally observed displacement of the symmetric vibrational mode A_g , have been compared with computer simulations. These have been performed at the local density approximation (LDA) density functional level using the Dmol³ package [17]. The LDA has proved to be more adequate than the generalized gradient approximation (GGA) for polyethylene [18]. The calculation has been carried out for four of the materials included in the series of ethylene/1-hexene copolymers. For each system geometry optimizations were performed taking into account constrains for “ a ” and “ b ” cell parameters. Subsequent vibrational analysis was performed to get all fundamental vibrational modes for polyethylene (Raman and IR modes). Intensity band calculation was not accessible by the software so Raman active symmetric deformation fundamental mode A_g has been to be deduced. First the motions of the vibrational modes have been animated with the help of the simulation software, isolating the four corresponding to the deformation modes [4, 19]. However, only two of them are active in Raman, one corresponding to the symmetric mode A_g and the other corresponding to anti-symmetric mode B_{3g} . These vibrations possess the inversion

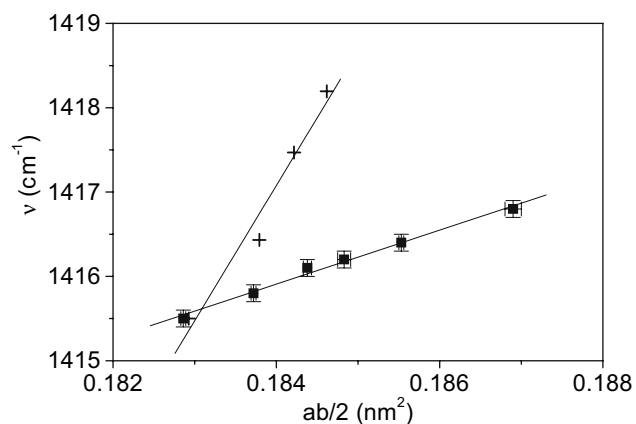


Fig. 3 Comparison of the experimental variation of the 1415 cm^{-1} band (squares) and the computer simulations (crosses). Simulated values have been shifted by a constant value taking as reference the linear PE sample. The lines are linear regressions of simulated and experimental values

centers at the midpoints of the C–C-bond ($g = \text{gerade}$) and the IR active deformation modes lack of them ($u = \text{ungerade}$).

It is known that the symmetric deformation mode A_g appears at a lower wavenumber than the anti-symmetric deformation mode B_{3g} , then we have selected the lower value of the two simulated active Raman modes, which appears in the linear PE sample at 1366 cm^{-1} . The simulated frequency data showed in Fig. 3 have been scaled so that the calculated value for the linear PE sample (1366 cm^{-1}) matched the experimental one (1415 cm^{-1}). As it can be seen both sets show a linear relationship with the cell expansion parameters, with a larger slope corresponding to the simulated data. It should be pointed out that infinite crystal size is supposed in the simulated systems due to the periodic conditions taken into account for the calculations. Those materials with greater 1-hexene content would probably have larger deviation from the simulation conditions, giving rise to larger differences between experimental and calculated frequencies. Moreover, the presence of Fermi resonance in the bending region could produce the displacement of CH_2 1415 cm^{-1} vibrational mode to a higher wavenumber. Simulated data do not keep in mind Fermi resonance coupling, being able to cause a drop in wavenumber of vibrational A_g modes.

Acknowledgements We acknowledge to M.T. Expósito for kindly supply some of the copolymers studied in this work. J. Otegui thanks the CSIC (Post-graduate I3P Program) for the tenure of a fellowship. J.F. Vega acknowledges the MEC for a Ramón y Cajal Tenure (2006). Thanks are due to the CICYT (MAT2006-0400 project) for financial support.

References

1. Strobl GR, Hagedorn W (1978) *J Polym Sci: Polym Phys Ed* 16:1181
2. Siesler HW, Holland-Moritz K (1980) *Infrared and Raman Spectroscopy of Polymers*. Marcel Dekker Inc., New York
3. Snyder RG, Scherer JR, Peterlin A (1981) *Macromolecules* 14:77
4. Bower DI, Maddams WF (1989) *The Vibrational Spectroscopy of Polymers*. University Press, Cambridge, U.K
5. Mutter R, Stille W, Strobl G (1993) *J Polym Sci: Polym Phys Ed* 31:99
6. Rull F, Prieto AC, Casado JM, Sobron F, Edwards HG (1993) *M J Raman Spectrosc* 24:545
7. Naylor CC, Meier RJ, Kip BJ, Williams KPJ, Mason SM, Conroy N, Gerrard DL (1995) *Macromolecules* 28:2969
8. Lagarón JM (2002) *J Mat Sci* 37:4101
9. Boerio FJ, Koenig JL (1970) *J Chem Phys* 52:3425
10. Snyder RG, Hsu SL, Krimm S (1978) *Spectrochim Acta* 34A:395
11. Abbate S, Zerbl O, Wunder SL (1982) *J Phys Chem* 86:3140
12. Swan PR (1962) *J Polym Sci* 56:409
13. Davies GT, Eby RK, Martin GM (1968) *J Appl Phys* 39:4973
14. Baltá Calleja FJ, González Ortega JC, Martínez de Salazar J (1978) *Polymer* 19:1094
15. Martínez de Salazar J, Baltá Calleja FJ (1979) *J Cryst Growth* 48:283
16. Lagarón JM, Powell AK, Davidson NS (2000) *Macromolecules* 33:1030
17. (a) Delley B (1990) *J Chem Phys* 92:508; (b) Delley B (2000) *J Chem Phys* 113:7756
18. Barrera GD, Parker SF, Ramírez-Cuesta AJ, Mitchell PCH (2006) *Macromolecules* 39:2683
19. Nielsen JR, Holland RF (1961) *J Mol Spectr* 6:394